Iris Biometric for Person Identification Using Dual- Tree Complex Wavelet Transform

Neelam T. Rakate, U. A. Patil

Abstract*— Technologies that exploit biometrics have the potential for application to the identification and verification of individuals for controlling access to secured areas or materials. A wide variety of biometrics has been marshaled in support of this challenge. Resulting systems include those based on automated recognition of retinal vasculature, fingerprints, hand shape, handwritten signature, and voice. Unfortunately, from the human factors point of view, these systems are highly invasive. One possible alternative to these methods that has the potential to be less invasive is automated iris recognition. Interestingly, the spatial patterns that are apparent in the human iris are highly distinctive to an individual. The iris has unique features and is complex enough to be used as a biometric signature. Therefore, in order to use the iris pattern for identification, it is important to define a representation that is well adapted for extracting the iris information content from images of the human eye. Here we represent a new algorithm for extracting unique features from images of the iris of the human eye and representing these features using two-dimensional dual-tree complex wavelet transform (DTCWT). This representation is then utilized to recognize individuals from images of the irises of their eyes. The proposed technique is translation & shift invariant. For the dual filter tree, we have selected two linear phase biorthogonal filter sets of same lengths (based on Selesnick's approach) which are used to filter each signal for quantization to 375 byte iris feature codes. Then the Hamming distance is used to match two iris codes. The experimental results on UPOL database shows good reliability and performance, so it is promising to be used in a personal identification system.

Index Terms*— Biometrics, Complex Wavelet Transform, Feature extraction, Hamming distance.

I. INTRODUCTION

As modern society increasingly depends on systems to provide secure environments and services to people, it becomes paramount to ensure the security of a system through means to identify the validity of an individual requesting access to it. This is usually established by extracting some form of information from the individual to check against information held by the system about valid users. Biometric refers to automatic identity authentication of a person on the basis of one's unique physiological or behavioral characteristics. Some of the popular biometrics that are used include fingerprint, face, iris, hand geometry, retina, signature, voice, gait, palm prints, etc. Among other biometric technologies, iris-based authentication systems bear more advantages than other biometric technologies do [1].

Manuscript received February, 2014.

Miss. Neelam T. Rakate, Department of Electronics Engineering, D.K.T.E, and society's Textile & Engineering Institute, Ichalkaranji, India.

Prof. U. A. Patil, Department of Electronics Engineering, D.K.T.E, and society's Textile & Engineering Institute, Ichalkaranji, India.

The iris is a delicate circular diaphragm, which lies between the cornea and the lens of human eye. Iris patterns are believed to be unique due to complexity of the environmental and genetic processes that influence the generation of iris pattern. These factors result in textural patterns that are unique to each eye of an individual and even distinct between twins. The iris is considered to be one of the most stable biometric, as it is believed to not alter significantly during a person's lifetime.

The purpose of Iris recognition is, it is a biometrical based technology for personal identification and verification, & its purpose is to recognize a person from his/her iris prints. The iris recognition technology combines computer vision, pattern recognition, statistical inference and optics. Its purpose is high confidence recognition of a person's identity by mathematical analysis of the random patterns that are visible within the iris of an eye from some distance. Image processing techniques can be employed to extract the unique iris pattern from a digitized image of the eye, and encode it into a biometric template, which can be stored in a database.

The process of information extraction starts by locating the pupil of the eye, which can be done using any edge detection technique. The centroid of the detected pupil is chosen as the reference point for extracting the features of the iris. Choosing the centroid as the reference point ensures that the representation is translation invariant. Since variations in the eye, like optical size of the iris, position of pupil in the iris, and the iris orientation change person to person, it is required to normalise the iris image so that the representation is common to all with similar dimensions. The feature code (iris code) which is extracted from feature extraction process is to be compared with the stored feature code for authentication. Based upon matching result, the decision is made with high confidence whether two codes are from the same iris or from two different irises.

In this paper, we have presented the algorithm for iris recognition based on dual tree complex wavelet transform and explore its accuracy and efficiency. The rest of the paper is organized as follows: section II deals with the iris recognition system, section III deals with the preprocessing of the iris images, section IV explains our proposed iris feature extraction and encoding approach using dual-tree complex wavelet transform, section V explains the matching technique, section VI shows the experimental results; and section VII is the conclusion.

II. IRIS RECOGNITION SYSTEM

A remarkable and important characteristic of the iris is the randomly distributed irregular texture details in all directions. The main idea behind this topic is to recognize a person by comparing his/her iris features with an iris feature database. A key and still open issue in iris recognition is how

Published By:
Blue Eyes Intelligence Engineering
& Sciences Publication Pvt. Ltd.

best to represent such textural information using a compact set of features (iris features) that will give the best matching results. To solve the problem defined above, here we have used a novel approach of feature extraction of iris image using 2-D Dual-Tree Complex Wavelet Transform (DTCWT). The main objective is to implement an open-source iris recognition system in order to verify both the uniqueness of the human iris and also its performance as a biometric. The development tool used is MATLAB, and emphasis will be only on the software for performing recognition, and not hardware for capturing an eye image. The iris recognition consists of image acquisition, iris segmentation, normalization, feature extraction and feature comparison as shown in Figure 1.

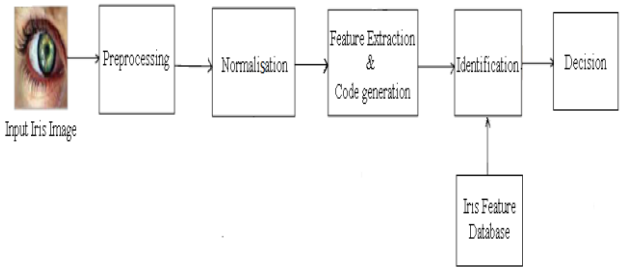

Fig 1: Block diagram of Iris Recognition System

In image acquisition, an image of the person's eye is obtained through standard databases & it is preprocessed in order to reduce noise using various digital filters. The initial stage deals with iris segmentation. This consists of localizing the iris inner (pupillary) and outer (scleric) borders. Then, iris boundary co-ordinates are converted to the stretched polar coordinates in order to normalize the scale and illumination of iris in the image. In feature extraction, features representing the iris patterns are extracted based on texture analysis using dual-tree complex wavelet transform by finding the singularities with phase information in 12 directions $\{-15^0, -30^0, -45^0, -60^0, -75^0, 0^0, 15^0, 30^0, 45^0, 60^0, 75^0, 90^0\}$ [3]. Iris features are obtained by computing energies and standard deviation of detailed coefficients in 12 directions. Finally, the person is identified by comparing his/her iris features with an iris feature database using Hamming distance technique.

III. IRIS PREPROCESSING

A. Database of Iris Images

There are two methods of iris image acquisition available:

a) Using Iris Cameras
b) Using available databases from internet

In this work, we are using available databases from internet. An image of the person's eye is obtained through various databases such as CASIA, BATH, UBIRIS, MMU, UPOL, ICE, WVU, etc. To enable the effective test of the proposed classification strategy, we have analyzed & selected the UPOL database by considering visibility of iris patterns. This database contains total 384 numbers of images for 64 persons. For each person, the selected database has 3 left eye images & 3 right eye images. These images are 24- bit RGB true color images, resolution is 768x576 pixels & file format is .png (Portable network group). These images were scanned by TOPCON TRC50IA device connected with SONY DXC-950P 3CCD camera. Figure 2 shows some of the UPOL database images.

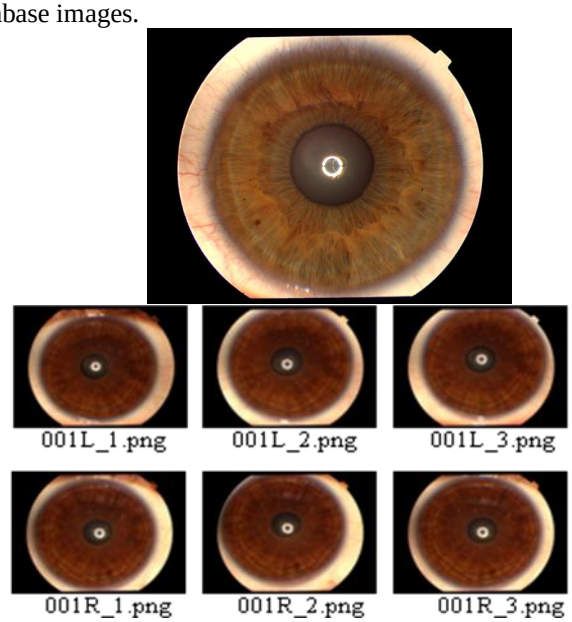

Fig 2: UPOL database images

B. Image manipulation

In the pre-processing stage, we transformed the images from RGB to gray level and from eight-bit to double precision thus facilitating the manipulation of the images in subsequent steps. The '*rgb2gray'* function is used to convert RGB images to grayscale by eliminating the hue & saturation information while retaining the luminance. This function converts RGB values to grayscale values by forming a weighted sum of the R, G & B components:
0.2989*R + 0.5870*G + 0.1140*B

C. Image Pre-processing

Image pre-processing is used to condition or enhance the input image in order to make it suitable for further processing. Pre-processing methods use a small neighborhood of a pixel in an input image to get a new brightness value in the output image. Such pre-processing operations are also called Filtration.

Noise is the result of errors in the image acquisition process that result in pixel values that do not reflect the true intensities of the real scene. There are different ways to remove or reduce noise in an image. As several images in database are contaminated by salt and pepper noise, we have selected standard 2-D median filter as reliable method to remove the salt and pepper noise without damaging the edge details. Figure 3 shows eye image taken in iris preprocessing & Figure 4 shows median filtered image.

Fig 3: Input eye image

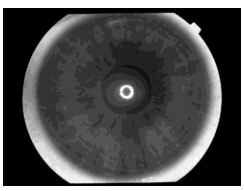

Fig 4: Median filtered image

Published By:
Blue Eyes Intelligence Engineering
& Sciences Publication Pvt. Ltd.

Median filtering is similar to using an averaging filter, in that each output pixel is set to an average of the pixel values in the neighborhood of the corresponding input pixel. However, with median filtering, the value of an output pixel is determined by the median of the neighborhood pixels, rather than mean. The median is much less sensitive than mean to extreme values (called outliers). Median filtering is therefore better able to remove these outliers without reducing sharpness of the image.

D. Image Localization

The part of the eye carrying information is only the iris part. It lies between the sclera and the pupil. Hence the next step after filtering the image is to separate the iris part from the eye image. Before performing iris pattern matching, the boundaries of the iris should be located. In other words, we are supposed to detect the part of the image that extends from inside the limbus (the border between the sclera and the iris) to the outside of the pupil. We start by determining the outer edge by using the canny operator with the default threshold value given by MATLAB, to obtain the gradient image. Canny Edge Detector finds edges by looking for the local maxima of the gradient of the input image. It calculates the gradient using the derivative of the Gaussian filter. The Canny method uses two thresholds to detect strong and weak edges [11]. It includes the weak edges in the output only if they are connected to strong edges. As a result, the method is more robust to noise, and more likely to detect true weak edges.

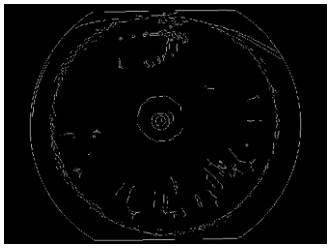

Fig 5: Canny Edge detected image

Canny edge detection algorithm goes through the following stages:

- Noise reduction.
- Finding the intensity gradient of the image.
- Non-maximum suppression.
- Tracing edges through the image and hysteresis thresholding.

E. Normalization

Once the iris region is segmented, the next stage is to normalize this part, to enable generation of the iris code and their comparisons. Since variations in the eye, like optical size of the iris, position of pupil in the iris, and the iris orientation change person to person [4], it is required to normalize the iris image so that the representation is common to all with similar dimensions. Normalization process involves unwrapping the iris and converting it into its polar equivalent as shown in Figure 6.

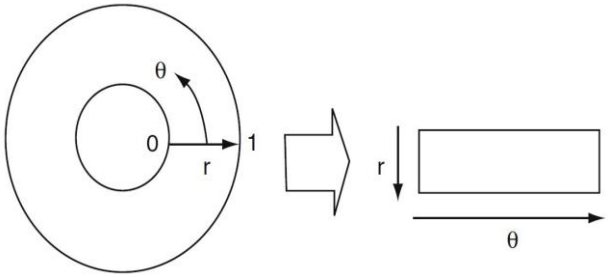

Fig 6: Generating normalized iris image.

The remapping of the iris region from the Cartesian coordinates to the normalized non-concentric polar representation is modeled as:

$$x = r\cos(\theta) \quad (1)$$

$$y = r\sin(\theta) \quad (2)$$

$$I(x(r, \theta), y(r, \theta)) \rightarrow I(r, \theta) \quad (3)$$

With:

$$x(r, \theta) = (1 - r)\, x_p(\theta) + r\, x_i(\theta) \quad (4)$$

$$y(r, \theta) = (1 - r)\, y_p(\theta) + r\, y_i(\theta) \quad (5)$$

Where $I(x, y)$ is the iris region image, (x, y) are the original Cartesian coordinates, (r, θ) are the corresponding normalized polar coordinates, and x_p, y_p and x_i, y_i are the coordinates of the pupil and iris boundaries along the θ direction.

For normalisation of iris regions a technique based on Daugman's rubber sheet model was employed. From the empirical study of the database, following parameters are found:

(a) Range of iris radii varies from 170 to 210 pixels.

(b) Range of pupil radii varies from 50 to 85 pixels.

Hence, to extract iris from eye image, we have taken approximate region of interest coordinates as: Radii of pupil=100 & radii of iris = 240. The centre of the pupil was considered as the reference point, and radial vectors pass through the iris region, as shown in Figure 7. A number of data points are selected along each radial line and this is defined as the radial resolution. The number of radial lines going around the iris region is defined as the angular resolution.

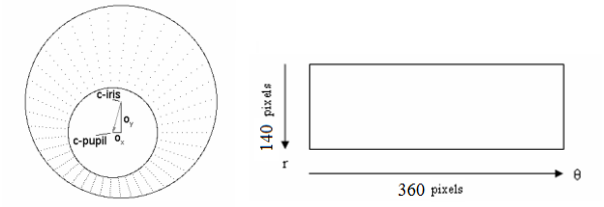

Fig 7: Outline of the normalisation process

However, the normalisation process was not able to perfectly reconstruct the same pattern from images with varying amounts of pupil dilation, since deformation of the iris results in small changes of its surface patterns.

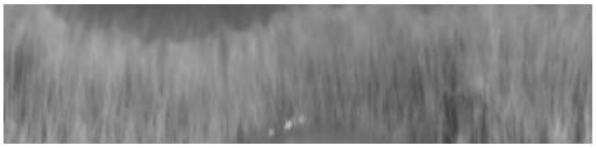

Fig 8: Normalised Iris Image

F. Histogram Equalization

This method usually increases the global contrast of many images, especially when the usable data of the image is

Published By:
Blue Eyes Intelligence Engineering
& Sciences Publication Pvt. Ltd.

represented by close contrast values. Through this adjustment, the intensities can be better distributed on the histogram. This allows for areas of lower local contrast to gain a higher contrast. Histogram equalization accomplishes this by effectively spreading out the most frequent intensity values.

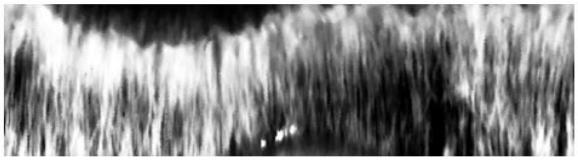

Fig 9: Histogram Equalized Image

IV. FEATURE EXTRACTION

In order to provide accurate recognition of individuals, the most discriminating information present in an iris pattern must be extracted. Most iris recognition systems make use of a band pass decomposition of the iris image to create a biometric template. For this we use wavelets transform, and more specifically the 2-D Dual-tree Complex Wavelet Transform.

A. Wavelet Transform

The need of simultaneous representation and localisation of both time and frequency for non-stationary signals (e.g. music, speech, images) led towards the evolution of wavelet transform from the popular Fourier transform. A wavelet has an oscillating wavelike characteristic but also has the ability to allow simultaneous time and frequency analysis and it is a suitable tool for transient, non-stationary or time-varying phenomena. Discrete-time and discrete-parameter version of wavelet transform is termed as Discrete Wavelet Transform (DWT Multilevel decomposition hierarchy of an image is illustrated in figure 10. Each decomposition breaks the parent image into four child images. These four child images are LL, LH, HL & HH wavelet coefficients [3]. Out of that only approximate coefficient LL is taken for next decomposition stage. Each of such sub-images is of one fourth of the size of a parent image. In this way, multilevel decomposition is done. The sub-images are placed according to the position of each subband in the two-dimensional partition of frequency plane.

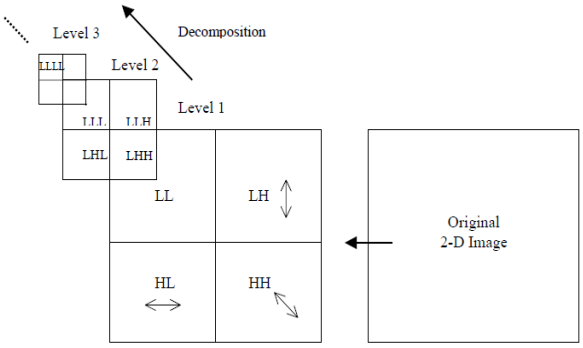

Fig 10: Multilevel decomposition hierarchy of an image with 2-D DT DWT

In spite of its efficient computational algorithm and sparse representation, the standard DWT suffers from four fundamental, intertwined shortcomings such as shift sensitivity, absence of phase information, oscillations, aliasing & poor directionality. All natural signals are basically real-valued, hence to avail the local phase information, complex-valued filtering is required. It is suggested in [13] the possibility of reducing two or more above-mentioned disadvantages using different forms of Complex Wavelet Transforms (CWT) with only limited (and controllable) redundancy and moderate computational complexity.

B. Complex Wavelet Transform

The initial motivation behind the earlier development of complex-valued DWT was the last limitation that is the absence of phase information. Complex Wavelets Transforms (CWT) use complex-valued filtering (analytic filter) that decomposes the real/complex signals into real and imaginary parts in transform domain. The real and imaginary coefficients are used to compute amplitude and phase information, just the type of information needed to accurately describe the energy localization of oscillating functions (wavelet basis).

The amplitude of these coefficients describes the strength of the singularity while the phase indicates the location of singularity. In order to determine the correct value of localised envelope and phase of an oscillating function, analytic or quadrature representation of the signal is used. This representation can be obtained from the Hilbert transform of the signal. An Analytic function is a complex valued function, constructed form a given real-valued function by its projections on real and imaginary subspaces (Hilbert space). The important property of an analytic signal is that its FT has single-sided spectral components.

C. Selesnick's Dual-tree Complex Wavelet Transform

In dual-tree CWT, two real wavelet trees are used as shown in Figure 11, each capable of perfect reconstruction (PR). One tree generates the real part of the transform and the other is used in generating complex part. For the dual trees, linear-phase perfect reconstruction biorthogonal filter sets should be selected & they should have good smoothness and rational coefficients [3]. It turns out that the implementation of the dual-tree complex wavelet transform requires that the first stage of the dual–tree filter bank be different from the succeeding stages. If the same PR i.e. perfect reconstruction filters are used for each stage, then the first several stages of the filter bank will not be approximately analytic; i.e. the frequency response for these stages will not be approximately single sided. Hence, in this algorithm, Farras filters are used in first stage and q-shift filters are used for higher three stages. All the filters used are of same length based on Selesnick's approach unlike Kingsbury's approach. There are various approaches to the design of filters for the dual-tree CWT. In the following, we describe methods to construct filters satisfying the following desired properties:

- Approximate half-sample delay property
- PR (Perfect Reconstruction)
- Orthogonal or biorthogonal - To preserve the energy in transform domain.
- Finite support (FIR filters)
- Vanishing moments/good stopband
- Linear-phase filters - To reduce the visually objectionable artifacts caused by nonlinear phase distortion. Selesnick's Dual- Tree Complex Wavelet Transform is shown in figure 11.

Published By:
Blue Eyes Intelligence Engineering
& Sciences Publication Pvt. Ltd.

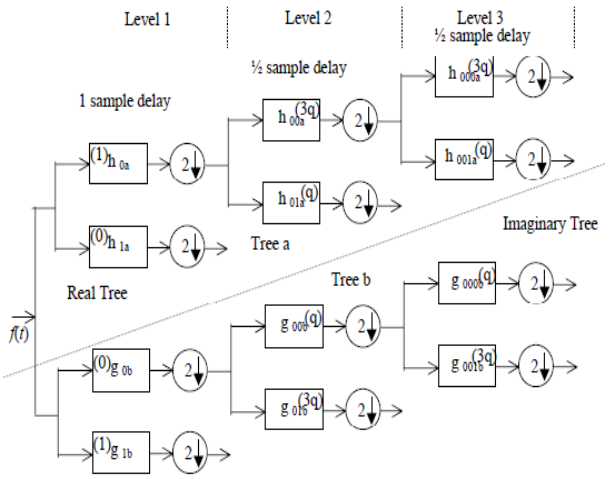

Fig 11: Selesnick's Dual- Tree Complex Wavelet Transform

As shown in above Fig-11, Tree a is implemented as real tree & Tree b is implemented as imaginary tree. The filters h_{0a} & h_{1a} are farras filters of first stage whereas h_{0a} is low pass filter & h_{1a} is high pass filter of real tree. Similarly, g_{0b} & g_{1b} are farras filters of first stage whereas g_{0a} is low pass filter & g_{1b} is high pass filter of imaginary tree. Similarly, for remaining stages 2, 3 & 4 q-shift high pass and low pass filters are implemented for both trees. To get uniform interval between the samples of both trees after level-1, filters in one tree must provide delays that are half a sample different from those in opposite tree. The half-sample delay condition is equivalent to uniformly oversampling the low-pass signal at each scale by 2:1, thus largely avoiding the aliasing due to the low-pass down samplers. Hence, half sample delay condition leads to a nearly shift-invariant wavelet transform. It has been shown that if filters in both trees be made to be offset by half-sample, two wavelets satisfy Hilbert transform pair condition and an approximately analytic wavelet is given by equation (6).

$$\psi(x)=\psi_h(x)+ j\psi_g(x) \qquad (6)$$

Where, $\psi(x)$ is complex wavelet and $\psi_h(x)$ and $\psi_g(x)$ are real wavelet and imaginary wavelet [1]. Dual-tree filters designed to satisfy the half-sample delay condition should not be used for the first stage. For the first stage, it is necessary only to translate one set of filters by one sample with respect to the other set. From equation (6) low pass filters, after the first stage and at first stage respectively are given by equation (7).

$$g_{00b}(n) = h_{00a}(n-0.5) \text{ and } g_{0b}(n) = h_{0a}(n-1) \qquad (7)$$

Similarly, high pass filters are given by equation (8).

$$g_{01b}(n) = h_{01a}(n-0.5) \text{ and } g_{1b}(n) = h_{1a}(n-1) \qquad (8)$$

Thus, the decomposition for each mode is performed in a standalone mode, in one after another stage i.e. total of 6 detailed coefficients are derived at each stage; three for the real tree and three for the imaginary tree. 4-stage decomposition is performed. At each stage, coefficients are oriented towards their respective directions as stated in following equations. Following six wavelets, as given by following six equations, are used to obtain oriented 2-D separable wavelets:

$$\psi_{1,1}(x,y) = \phi_h(x)\psi_h(y) \qquad \psi_{2,1}(x,y) = \phi_g(x)\psi_g(y)$$
$$\psi_{1,2}(x,y) = \psi_h(x)\phi_h(y) \qquad \psi_{2,2}(x,y) = \psi_g(x)\phi_g(y)$$
$$\psi_{1,3}(x,y) = \psi_h(x)\psi_h(y) \qquad \psi_{2,3}(x,y) = \psi_g(x)\psi_g(y) \qquad (9)$$

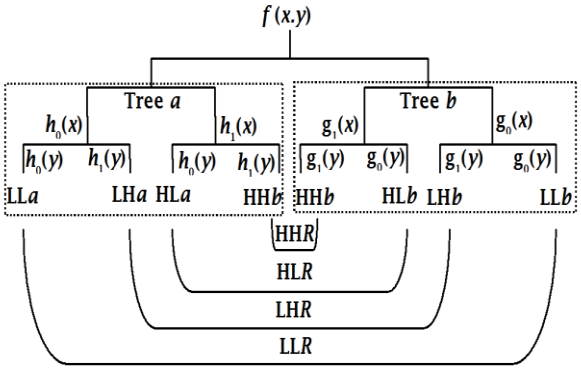

Fig 12: Formation of Real Tree DT CWT

where, $\psi_{1,i}$ correspond to the coefficients derived from the real tree and $\psi_{2,i}$ correspond to the coefficients derived from the imaginary tree. They can be combined to form complex wavelet coefficients as shown:

$$\Psi_i(x,y) = \frac{1}{\sqrt{2}}\left(\Psi_1,i(x,y) - \Psi_2,i(x,y)\right),$$
$$\Psi_{i+3}(x,y) = \frac{1}{\sqrt{2}}\left(\Psi_1,i(x,y) + \Psi_2,i(x,y)\right) \qquad (10)$$

Normalization by $\frac{1}{\sqrt{2}}$ is used so that the sum difference operation constitutes an orthonormality [2]. These six wavelet sub-bands of the 2-D DT-CWT are strongly oriented in {+15°,+45°,+75°, -15°, -45°, -75°} direction as shown in Figure 13 by red lines and it captures image information in those directions. Thus, in particular, 2D dual-tree wavelets are not only approximately analytic but also oriented.

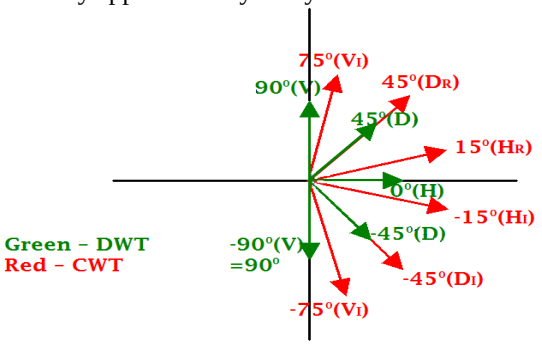

Fig 13: Orientations of sub-bands of DWT, CWT

Based on the coefficients, we generate an image of size 9*23 giving a feature code of 375 bytes called as iris code shown in Figure 14. This iris code is use for matching.

Fig 14: Feature extraction image

V. MATCHING

The last module of an iris recognition system is used for matching two iris templates. Its purpose is to measure how

Published By:
Blue Eyes Intelligence Engineering
& Sciences Publication Pvt. Ltd.

similar or different the templates are and to decide whether they belong to the same individual or not. An appropriate match metric can be based on direct point-wise comparisons between the phase codes. The test of matching is implemented by the XOR operator that is applied to the encoded feature vector of any two iris patterns [5]. The XOR operator detects disagreement between any corresponding pair of bits. The system quantifies this matter by computing the percentage of mismatched bits between a pair of iris representations, i.e., the normalized Hamming distance. Let X and Y are two iris templates to be compared and N is the total number of bits so, HD (Hamming Distance) is equal to the number of disagreed bits divided by N as shown in equation (11).

$$HD = \frac{1}{N}\sum_{j=1}^{N} X_j \oplus Y_j \quad (11)$$

The smallest HD value amongst all these values is selected, which gives the matching decision. If the distance obtained is below a predefined threshold level, the studied sample is considered to belong to the user whose template is being studied. Selection of the threshold level usually depends on the final application. Hamming distance offers the best results for this biometric modality and the selected algorithm. The HD value generally varies from 0.25 to 0.35 under single false match probabilities.

VI. RESULTS

A. *Flowchart of the System*

The proposed system consists of two flowcharts. One for user enrolment and other for user authentication.

User Enrolment mode: In the user enrolment process, image of eye is taken from iris database. It is then processed through all the steps such as Image segmentation, localization, normalization, code generation for further authentication. Once the template is obtained, it is stored as .MAT (binary) file in MATLAB software. As UPOL database provides three left eye & three right eye images for every person, we have created binary templates for L_1 image i.e. left eye first image & another biometric template for R_1 image i.e. right eye first image. Such binary templates are stored under one structure variable which is then represented as feature database. Hence, by repeating the same procedure we can get binary templates for 'n' number of users which are stored in feature database.

User Authentication mode: The user authentication system does a similar job as done in user enrolment process i.e. processing of iris image. In the identification process, the system generates the biometric template from the trainee eye image and compares that against the stored feature database. Identification is typically based on Hamming Distance criteria. If the hamming distance obtained is below a predefined threshold level, the studied sample is considered to belong to the user whose template is being studied, otherwise that user is invalid.

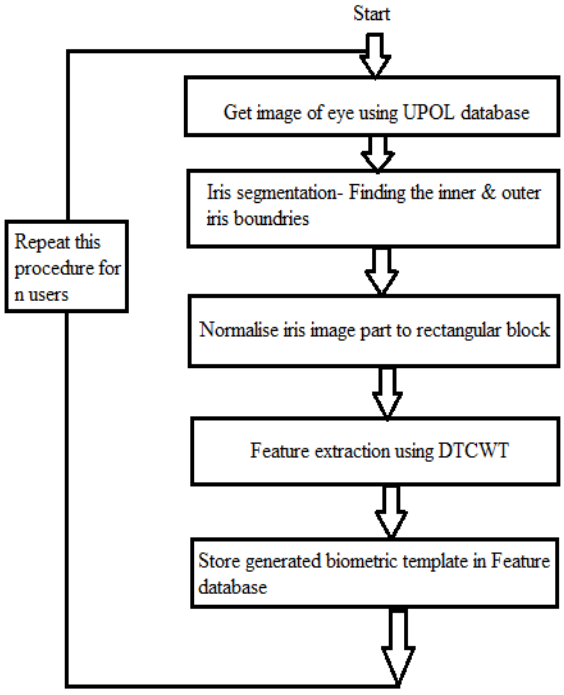

Fig 15: Flowchart for User Enrolment

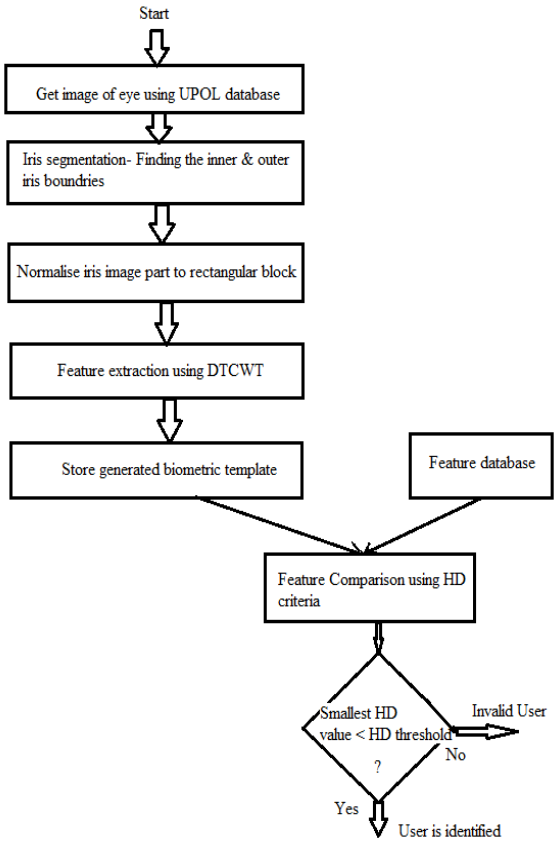

Fig 16: Flowchart for User Authentication

B. *Experimentation*

In this work, UPOL Database is used for testing and result generation. Firstly, we have converted RGB images to grayscale images & further processing such as noise removal, iris segmentation, normalization & feature extraction is done to grayscale images. From the empirical study of the database, following parameters are found:

(a) Range of iris radii varies from 170 to 210 pixels.

(b) Range of pupil radii varies from 50 to 85 pixels.

Published By:
Blue Eyes Intelligence Engineering
& Sciences Publication Pvt. Ltd.

Hence, to extract iris from eye image, we have taken approximate region of interest (ROI) coordinates as: Radii of pupil=100 & radii of iris = 240. After segmentation, normalized image we are getting is 140x360 pixels. Normalized image is subjected to feature extraction using dual-tree complex wavelet transform technique. The feature code (iris code) that is extracted from feature extraction process is to be compared with the stored feature code for authentication.

C. Results

In this work, we have prepared database or enrolment for 64 persons by taking their left eye first images e.g. 001L_1 & also right eye first images e.g 001R_1. Hence, created .MAT (binary) files using MATLAB computational engine. Table 1 represents results table giving Accuracy of the system. As we have created binary templates for left eye as well as right eye of the same person, we can treat these templates as two different persons because as per medical considerations, persons left & right eye does not have same iris patterns. In this work, for left & right eye images of the same person, this system is giving up to 92.25% of mismatch results.

D. Performance Evaluations

The performance of a biometric authentication system can be measured as the False Acceptance Rate (FAR), or the False Rejection Rate (FRR) which are defined as:

$$FAR = \frac{\text{number of false acceptances}}{\text{number of client accesses}}$$

$$FRR = \frac{\text{number of false rejections}}{\text{number of client accesses}} \quad (12)$$

That is, FAR is the probability that a non-authorized person is identified. FRR is the probability that an authorized person is not identified; FIR (False Identification rate) is the probability that an authorized person is identified but is assigned to false id value. A perfect biometric authentication system would have a FRR = 0 and a FAR = 0 which is a little bit unachievable in reality. It is also interesting that any of the two values FRR and FAR can be reduced to an arbitrary small number, with the drawback of increasing the other value. The FAR/FRR curve pair is excellently suited to set an optimal threshold for the biometric system. The Receiver Operating Characteristic (ROC), which plots FRR values directly against FAR values, thereby eliminating threshold parameters. The ROC, like the FRR, can only take on values between 0 and 1 and is limited to values between 0 and 1 on the x axis (FAR). Table 2 represents results giving FAR, FRR & FIR of the system.

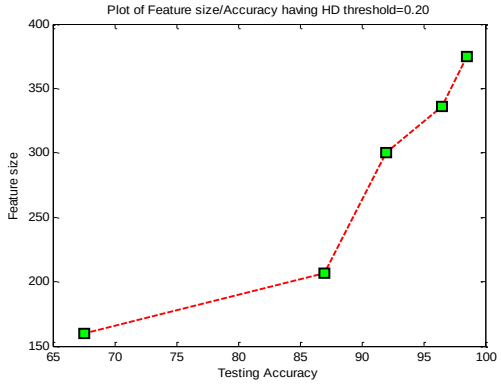

Fig 17: Plot of Feature size vs. Accuracy having HD threshold=0.20

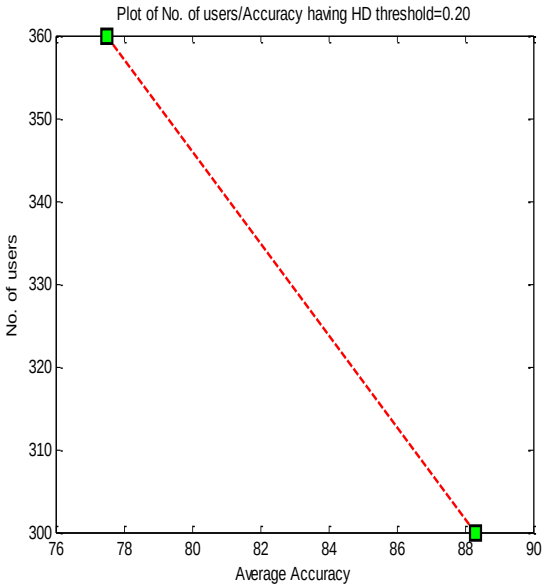

Fig 18: Plot of Number of users vs. Accuracy having HD threshold=0.20

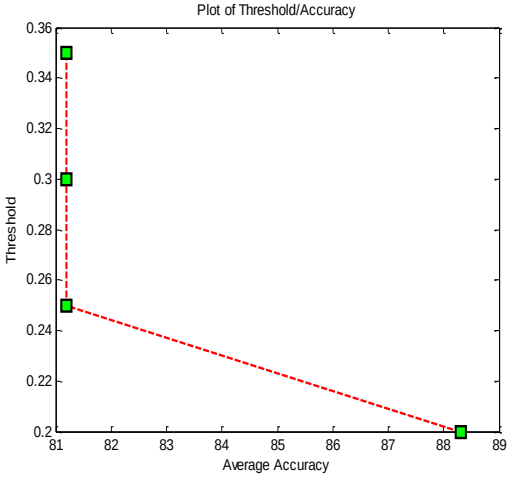

Fig 19: Plot of Threshold vs. Accuracy

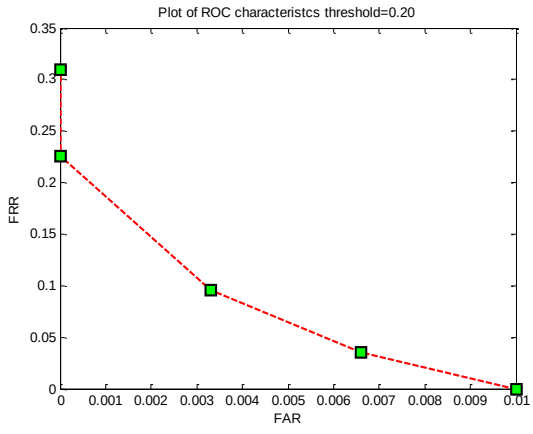

Fig 20: Plot of ROC characteristics having HD threshold=0.20

VII. CONCLUSION

The conclusions drawn from results given by algorithm used for feature extraction of iris part of eye image in prototype system design using image processing approach are as follows:

1. An image processing approach for iris feature code generation using dual-tree complex wavelet transform has been implemented.

Published By:
Blue Eyes Intelligence Engineering
& Sciences Publication Pvt. Ltd.

2. The designed system provides best results for approximate ROI co-ordinates: radii of pupil=100 & radii of iris = 240.
3. The radial and angular resolution, r =141 and θ = 0^0-360^0 respectively, which gives the number of data points for encoding each template.
4. The filter parameters used for feature encoding satisfies Half- sample delay condition, Perfect reconstruction (orthogonality or biorthogonality), Linear phase finite impulse response, good stopband/ Vanishing moments, etc properties. Hence, we have selected Farras filters (for first stage) & Q- shift filters (for remaining stages).
5. From result table, for single iris biometric template in feature database gives 100% false matches for 381 trainee iris images & 100% accurate matches for 3 test iris images which are belonging to same person.
6. For the two iris templates generated from the same iris, have a Hamming distance of 0.0 exactly.
7. For 100 biometric templates in feature database, with Hamming distance threshold of 0.20, system gives average testing accuracy 88.30% and that of for HD threshold of 0.25 system gives average testing accuracy 81.20%. This means that system gives a better performance at 0.20 HD threshold value.
8. From figure 18, we can conclude that, for 120 biometric templates in feature database with Hamming distance threshold of 0.20, the system gives average testing accuracy 77.50% which are somehow poor results than that for 100 biometric templates giving average testing accuracy of 88.30% for same HD threshold. This means that as the number of persons (i.e. biometric templates) increases in feature database, the system gives poor results because many of feature comparisons gives a very closer values of Hamming distance & hence sometimes it gives false matching results.
9. From figure 17, it has been observed that, as feature size increases, accuracy also increases. In this thesis, we have calculated results for 5 feature sizes 375 bytes, 336 bytes, 300 bytes, 207 bytes & 160 bytes.
10. From figure 19, it has been observed that, as HD threshold value increases beyond 0.25, accuracy remains same.
11. It has been observed that, optimum HD threshold value is 0.20. As the ROC curves lie very near the coordinate axis, indicates that system has good performance characteristics.
12. From this, we can conclude that, maximum number of persons or biometric templates handled by system are 110 which are giving 91% average accuracy.
13. For left & right eye images of the same person, this system is giving up to 92.25% of mismatch results that represents good measure for biometric identification.
14. Experimental results showed that the above algorithm based on DTCWT have demonstrated the effectiveness of the proposed method in terms of improving the recognition rate as compared older methods.
15. Inherent shift invariance is the added advantage of this method. This shows that our approach is promising to improve iris based identification.

REFERENCES

[1] A. S. Narote, S. P. Narote, L. M. Waghmare and M. B. Kokare, "Robust iris feature extraction using dual tree complex wavelet transform," 2007, IEEE International Conference on Signal Processing and Communications (ICSPC 2007), 24-27 November 2007, Dubai, United Arab Emirates.

[2] Waheeda Almayyan , Hala S. Own, Hussein Zedan, "Iris Features Extraction using Dual-Tree Complex Wavelet Transform," International Conference of Soft Computing and Pattern Recognition 2010.

[3] Ivan W. Selesnick, Richard G. Baraniuk, and Nick G. Kingsbury, "The Dual-Tree Complex Wavelet Transform," IEEE Signal processing magzine, pp.: 123-152, November 2005.

[4] Rajesh M. Bodade, Dr. Sanjay N. Talbar, "Iris Recognition using Combination of Dual Tree Rotated Complex Wavelet and Dual Tree Complex Wavelet," IEEE ICC 2009 proceedings.

[5] J. Daugman, "High Confidence Visual Recognition of Persons by a Test of Statistical Independence," IEEE Trans. on Pattern Analysis and Machine Intelligence, Vol. 15, No.11, pp.1148-1161, 1993.

[6] G Kaiser, "A Friendly Guide to Wavelets", Birkhauser, Boston, 1994.

[7] W Lawton, "Applications of Complex Valued Wavelet Transforms to Subband Decomposition", IEEE Trans. Sig. Proc., 41, 12, 3566-3568, 1993.

[8] X P Zang, M Desai, and Y N Peng, "Orthogonal Complex Filter Banks and Wavelets: Some Properties and Design", IEEE Trans. Sig. Proc., 47, 4, 1999.

[9] J. Daugman, "How Iris Recognition Works", IEEE Transactions on Circuits and Systems for Video Technology, vol. 14, no. 1, pp. 21-30, 2004.

[10] Mohammed A. M. Abdullah, F. H. A. Al-Dulaimi, Waleed Al-Nuaimy, Ali Al-Ataby, "Smart card with iris recognition for high security access environment", 978-1-4244-7000-6/11, IEEE 2011.

[11] John Canny, "A Computational Approach to Edge Detection", IEEE Transactions on Pattern Analysis and Machine Intelligence, Vol. PAMI-8, No. 6, November 1986.

[12] G. Annapoorani, R. Krishnamoorthi, P. Gifty Jeya, S. Petchiammal@Sudha, "Accurate and Fast Iris Segmentation", G. AnnaPoorani et al. / International Journal of Engineering Science and Technology, Vol. 2(6), 2010, 1492-1499.

[13] David Salomon, "Data Compression the complete reference", fourth edition, Springer publication.

Ms. Neelam. T. Rakate received the B.E. degree in Electronics & Telecommunication engineering in 2010 & is currently working toward the M. E. degree in Electronics at DKTE, Ichalkaranji. Her main areas of research interest are digital signal processing & image processing.

Prof. U. A. Patil received the M.E. degree in Electronics engineering from WCE, Sangli. In 2003, he joined Department of E & TC Engineering at DKTE Ichalkaranji as an Assistant Professor. His main areas of research interest are signal processing, wireless communication & networking.

Published By:
Blue Eyes Intelligence Engineering
& Sciences Publication Pvt. Ltd.

Sr. No	Feature Size (in bytes)	Feature Vector size	No. Of Persons in database	HD threshold	Total No. Of Images	Accuracy in %	
						Training	Testing
1	207	9*23	1	0.20	384	100	100
2	375	15*25	100	0.20	300	100	98.50
3	336	14*24	100	0.20	300	100	96.50
4	300	12*25	100	0.20	300	100	92.00
5	207	9*23	100	0.20	300	100	87.00
6	160	10*16	100	0.20	300	100	67.50
7	375	15*25	100	0.25	300	100	92.50
8	336	14*24	100	0.25	300	100	87.00
9	300	12*25	100	0.25	300	100	82.50
10	207	9*23	100	0.25	300	100	77.50
11	160	10*16	100	0.25	300	100	66.50
12	375	15*25	120	0.20	360	100	86.25
13	336	14*24	120	0.20	360	100	82.50
14	300	12*25	120	0.20	360	100	80.83
15	207	9*23	120	0.20	360	100	73.33
16	160	10*16	120	0.20	360	100	64.58

Table 1: Results giving Accuracy of the system

Published By:
Blue Eyes Intelligence Engineering
& Sciences Publication Pvt. Ltd.

Sr. No	Feature Size (in bytes)	No. Of Persons in database	HD threshold	Total No. Of Images	FAR	FRR	FIR
1	375	100	0.20	300	0.00%	0.99%	0.00%
2	336	100	0.20	300	3.57%	0.66%	1.67%
3	300	100	0.20	300	9.52%	0.33%	5.00%
4	207	100	0.20	300	22.61%	0.00%	8.66%
5	160	100	0.20	300	31.00%	0.00%	21.66%

Table 2: Results giving FAR, FRR & FIR of system

Published By:
Blue Eyes Intelligence Engineering
& Sciences Publication Pvt. Ltd.